

The local density of matter mapped by *Hipparcos*

Johan Holmberg¹ and Chris Flynn²

¹ *Lund Observatory, Box 43, SE-22100 Lund, Sweden*

² *Tuorla Observatory, Väisäläntie 20, FI-21500, Piikkiö, Finland*

Accepted 1999 June 16. Received 1999 May 19; in original form 1998 December 30

ABSTRACT

We determine the velocity distribution and space density of a volume complete sample of A and F stars, using parallaxes and proper motions from the *Hipparcos* satellite. We use these data to solve for the gravitational potential vertically in the local Galactic disc, by comparing the *Hipparcos* measured space density with predictions from various disc models. We derive an estimate of the local dynamical mass density of $0.102 \pm 0.010 M_{\odot} \text{pc}^{-3}$, which may be compared to an estimate of $0.095 M_{\odot} \text{pc}^{-3}$ in visible disc matter. Our estimate is found to be in reasonable agreement with other estimates by Crézé et al. (1998) and Pham (1997), also based on *Hipparcos* data. We conclude that there is no compelling evidence for significant amounts of dark matter in the disc.

Key words: Galaxy: kinematics and dynamics – (Galaxy:) solar neighbourhood – Galaxy: structure – dark matter

1 INTRODUCTION

The European Space Agency’s *Hipparcos* satellite has produced very accurate distances and proper motions for a complete set of nearby stars. These data permit a reassessment of the amount of matter in the local Galactic disc because of two significant improvements. Firstly, the kinematics and vertical density distribution of stars used to trace the disc potential can be determined with much higher accuracy, permitting a better determination of the total amount of gravitating matter in the local disc. Secondly, *Hipparcos* improves the measurement of the local Luminosity Function, so that the amount of matter in the disc in visible components can be better estimated. Both these improvements lead to a better evaluation of any difference between the amount of visible disc matter (in gas and dust, stars, stellar remnants and sub-stellar objects) and the total amount of gravitating matter.

Any difference between these quantities would imply that there remain mass components in the disc which have not yet been directly observed, i.e. disc dark matter. The first proposal that there might be a lot of such unobserved matter dates to Oort (1932, 1960). Oort used the now classical method of solving the combined Poisson-Boltzmann equations for the kinematical and density distribution of a population of stars, assumed to be stationary in the total matter distribution of the disc. Oort found that approximately one third of the local disc mass remained unaccounted for. Modern studies can arguably be dated from the work of Bahcall (1984a,b,c) who introduced a new method

of describing the visible disc matter as a series of isothermal components, in a reanalysis and corroboration of Oort’s results.

Studies since 1984 fall into two types, with mildly conflicting results. Firstly, the measurement of the kinematics and vertical density falloff in the disc of a stellar tracer (with the important improvement that both are determined from a single sample) from which the local volume density and/or local column density of matter in the disc may be derived. Kuijken & Gilmore (1989a,b,c), Kuijken (1991) found little evidence for disc dark matter using faint K dwarfs at the South Galactic Pole (SGP), whereas Bahcall, Flynn & Gould (1992), using bright K giants at the SGP, confirmed Bahcall’s (1984) claim of dynamically significant disc dark matter (over 50 per cent by mass) although with weakened statistical significance. The inclusion of the kinematics and local density of nearby K giants by Flynn & Fuchs (1994) to the sample of Bahcall et al. (1992) reduced the discrepancy between visible and total matter; they derived best fits with only 20 per cent of the disc mass in dark form. Secondly, general star counts in combination with mass models of the Galaxy may be used to infer the amount of disc dark matter. Bienaymé, Robin & Crézé (1987), in a study of star counts to faint magnitudes, found that the data could be well fitted by considering the mass distribution of the known matter only.

Very recently Crézé et al. (1998) have used the results from the *Hipparcos* mission to measure the kinematics and vertical falloff of complete samples of nearby A-F stars. The determination of the local density of gravitating matter then

arXiv:astro-ph/9812404v2 1 Nov 2005

proceeds via the Poisson-Boltzmann equations for the density of a tracer component in a self-gravitating disc. Only for A and F type stars does the density change sufficiently with vertical distance z from the disc mid-plane that the total local density of matter can be measured. The very great improvement comes because the distances to the tracer stars are measured directly for a complete sample via parallaxes, rather than via photometric methods as has always been the case before *Hipparcos*. They find that no dark matter is required in the local disc, measuring the total amount of gravitating matter as $\rho_0 = 0.076 \pm 0.015 M_\odot \text{pc}^{-3}$ while the amount of visible matter is estimated to lie in the range $\rho_{\text{vis}} = [0.06, 0.10] M_\odot \text{pc}^{-3}$.

Another study using *Hipparcos* data was made by Pham (1997), who used a different method to study F stars, where he determined scale heights and velocity dispersions for his chosen sample and then, assuming isothermality, used the $2\pi Gh_z^2 \rho_0 = \sigma_z^2$ relation. He finds the local mass density to be $\rho_0 = 0.11 \pm 0.01 M_\odot \text{pc}^{-3}$.

In this paper we have also used A-F stars in the *Hipparcos* catalogue to measure the local density of matter ρ_0 , using an analysis which differs somewhat from that of Cr ez e et al. (1998) and Pham (1997). We confirm the Cr ez e et al. (1998) and Pham (1997) result of little significant disc dark matter. We use the method of von Hoerner (1960) as described by Flynn & Fuchs (1994), in which the velocity distribution of a tracer population at the mid-plane may be integrated in a model of the local disc potential to yield its density falloff in the vertical direction. The predicted falloff may then be compared with the *Hipparcos* measured falloff, and the disc model evaluated. As is usual, our disc models describe the density stratification of known and putative dark components in the disc.

In section 2 we describe the selection of the sample from *Hipparcos*. In section 3 we detail our models of the disc mass stratification, and in section 4 we fit the data with and without dark matter in the models, finding it unnecessary to invoke disc dark matter. In section 5 we summarize and conclude.

2 THE HIPPARCOS CATALOGUE AND SELECTION OF SAMPLE

In order to measure the local density of matter, we require the vertical kinematics (i.e. w_0 velocity distribution at the Galactic midplane, $f(|w_0|)$) and the vertical density law $\nu(z)$ of a suitable tracer population. *Hipparcos* parallaxes may be used to estimate distances of tracer stars up to 200 pc. Only A and F stars develop a useful change in the density as a function of height z above the plane within 200 pc, so it is to these stars we confine our study.

The stars are drawn from the *Hipparcos* Survey (hereafter the ‘‘Survey’’), a predefined part of the *Hipparcos* Catalogue intended to be a complete, magnitude limited stellar sample. For stars of spectral type earlier than or equal to G5 this magnitude limit is $V \leq 7.9 + 1.1 \sin |b|$.

We select the A-F stars as follows. We select Survey stars with $-0.2 < B - V < 0.6$ and apply an absolute magnitude cut of $0.0 < M_V < 2.5$. These cuts are illustrated in Fig. 1. This results in 14342 stars. Proper motions and parallaxes are available for all these stars. We further divide

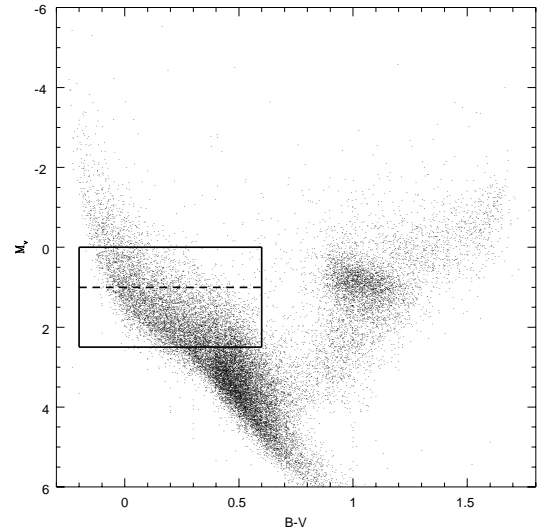


Figure 1. Hertzsprung-Russell diagram of *Hipparcos* survey stars with $\sigma_\pi/\pi < 15$ per cent. The sample used in this study is confined within the box. The dashed line divide the stars into the ‘‘A’’-star (above the line) and ‘‘F’’-star sample.

this sample into two at an absolute magnitude $M_V = 1.0$. We refer to these two samples as A and F stars. The first sample roughly takes in B5 to A5 stars, while the second covers A0 to F5 as a result of the rather large dispersion in the absolute magnitude to spectral type relation shown by *Hipparcos* (Houk et al. 1997; Jaschek & G omez 1998).

The vertical velocity dispersion of stars changes quite quickly as a function of absolute magnitude along the upper main sequence, as a consequence of the age-velocity relation (Wielen 1977). For this reason, dividing the sample into A and F makes the analysis of the velocity-density information in *Hipparcos* considerably simpler. Furthermore, since the A star sample is likely to be considerably younger than the F star sample, there is a possibility that the stars are so young that they are not yet fully mixed into the Galactic potential, a key assumption in applying the method. By working with an A and an F star sample we have some chance of detecting such effects. Ideally, one would prefer to be using old stars, such as dwarfs below the turnoff or K giants. We cannot use the dwarfs since they are well below the faintness limit of the Survey part of *Hipparcos*. The K giants develop only a small change in density with vertical distance within 200 pc.

The A star sample contains 4448 stars. We remove stars further than 200 pc, leaving 2026 stars. The F star sample contains 9894 stars. These stars are intrinsically fainter than the A stars, and we must apply a 100 pc distance limit in order to ensure that the sample remains complete. Applying this cut leaves 3080 stars.

For these two samples we use the *Hipparcos* proper motions and parallaxes to determine the distribution of vertical velocity and change in density with height, described in the next two subsections.

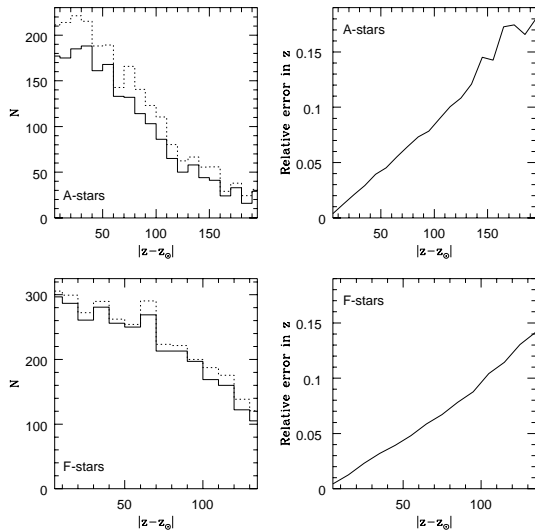


Figure 2. Lefthand panels show the number of stars in 10 pc slices in the samples before (solid) and after (dotted) corrections for distance measurement errors and reddening for A-stars (upper panel) and F-stars (lower panel). The righthand panels show the relative vertical distance error as a function of distance to the sun, $z - z_{\odot}$, for the two samples.

2.1 Stellar density laws

The density distribution of the tracer samples as a function of vertical distance from the galactic plane is determined within a cylinder centered on the sun. The radius of the cylinder is 100 pc for the F-star sample, and 200 pc for the A-star sample. Galactic (x, y, z) coordinates are determined for each star from the parallax and position on the sky, and the number of stars in 10 pc slices in z is determined. These samples are sufficiently local that the effects of dust absorption are very minor. We correct for extinction effects using the extinction model of Hakkila et al. (1997), which is a synthesis of a number of published studies.

The number density falloff and mean distance error as a function of vertical distance from the Sun $|z - z_{\odot}|$ is shown for the A-stars in the upper panels of Fig. 2 and for the F-stars in the lower panels. For most of the bins, the error in the distances to the stars is much less than the bin width, meaning that corrections to the observed density are small. For the A-stars the reddening correction has a larger impact than the distance errors, but only results in a change of the normalization of the counts and does not effect the slope, which is what we are concerned with here. To illustrate this, the solid histograms in the left panels show the observed density law in $|z - z_{\odot}|$, while the dotted lines show the extinction corrected density law. The corrections have been calculated using Monte-Carlo methods, in which large numbers of stars are simulated on the sky using the galactic model of Holmberg, Flynn & Lindegren (1997). We simulate the observation of stars by *Hipparcos* in the models, including the errors as a function of apparent magnitude and position on the sky, and this allows us to calculate the small correction between the observed and true density.

2.2 Vertical velocity distribution

Hipparcos gives us for the first time large numbers of accurate parallaxes and proper motions for a kinematically unbiased sample. Unfortunately, the original plan to obtain complementary radial velocities measurements was not implemented although the situation will improve in the near future (Udry et al. 1997). Full space velocities (u, v, w) are unobtainable for most of the stars, and any subsample of stars that have radial velocities would be kinematically biased towards high velocity stars. To get an unbiased estimate of the vertical velocities w we sacrifice the radial velocity information and work exclusively with the *Hipparcos* parallaxes and proper motions.

We use the standard galactic triad with principal directions \hat{x} towards the Galactic centre, \hat{y} in the direction of Galactic rotation, and \hat{z} towards the north Galactic pole, μ_{ℓ} and μ_b denoting the proper motions in galactic longitude and latitude in mas, π the parallax in mas and $\kappa=4.7405$ the numerical factor that gives V_T in km^{-1} . The tangential velocity of a star in the plane of the sky is then defined by

$$\mathbf{V}_T \equiv \frac{\kappa}{\pi} \begin{bmatrix} \sin \ell \cos b \mu_{\ell} - \cos \ell \sin b \mu_b \\ \cos \ell \cos b \mu_{\ell} - \sin \ell \sin b \mu_b \\ \cos b \mu_b \end{bmatrix} \quad (1)$$

The tangential velocity can also be written in terms of the space velocity \mathbf{v} (with \mathbf{e} giving the direction to the star) as

$$\mathbf{V}_T = \mathbf{v} - \mathbf{v}_R = \mathbf{v} - e v_R = \mathbf{v} - e e' v = (\mathbf{I} - \mathbf{u} \mathbf{u}') \mathbf{v} \quad (2)$$

Combining this we get the equation for the vertical velocity towards the north Galactic pole

$$w = \frac{\kappa \mu_b}{\pi \cos b} + u \cos l \tan b + v \sin l \tan b \quad (3)$$

The ensemble of tracer stars then gives an estimate of the vertical velocity distribution function $f(|w_0|)$. Ideally, one would like to determine $f(|w_0|)$ from the proper motions of all the stars in the two samples. We found it more practical to determine $f(|w_0|)$ from stars at low Galactic latitude, since we use proper motions for the stars and ignore the (incomplete) radial velocity data for the sample and the velocity distribution function is dominated by the proper motions rather than the unknown radial velocity at low Galactic latitude. We chose to use a Galactic latitude cutoff of $|b| < 12^\circ$. The choice of 12° galactic latitude was the best compromise between obtaining more stars by going to higher latitudes, while keeping $|b|$ low in order to minimize the effect of the unknown radial velocity on $f(|w_0|)$.

There are several error sources that affect the velocity distribution function, $f(|w_0|)$. An obvious one is that what we are measuring is not the distribution at the plane $f(|w_0|)$ but the mean of the distribution $f(|w|)$ within the region delimited by $|b| < 12^\circ$. Since samples taken further away from the plane are more dominated by kinematically hotter stars, this effect widens the velocity distribution. Another effect stems from measurement errors in the parallaxes — these scatter into the sample more distant stars. These stars must, in order to meet the apparent magnitude limit of the survey, be more luminous and hence younger and kinematically colder, which would narrow the velocity distribution. Finally, we are only measuring the part of the vertical velocity that comes from the proper motion in latitude. However,

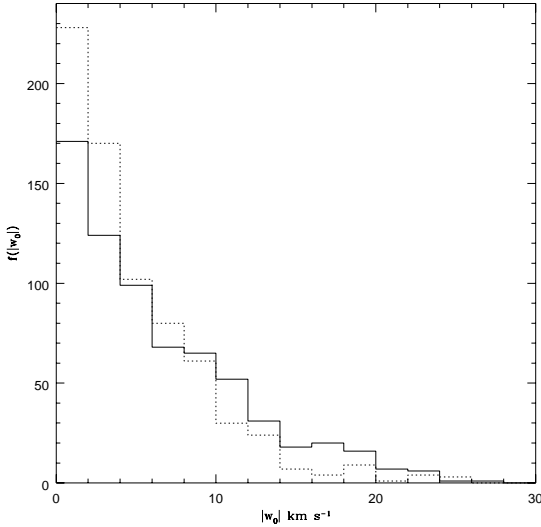


Figure 3. Histograms of vertical velocity at the plane, $f(|w_0|)$, for the A-star (dotted) and F-star (solid) samples.

this is the smallest error of the three. From studies of the effect on $f(|w_0|)$ of varying $|b|$ and the distance limit of the sample in simulated *Hipparcos* catalogues we estimate that the combined effect from these errors are of the order of 0.1 km s^{-1} for the A-sample, and even smaller for the F-sample, at a cutoff latitude of $|b| < 12^\circ$. For $|b| < 20^\circ$ the correction rises to 0.5 km s^{-1} which would eventually lead to a 20 per cent error in the estimated local density of the disc. For $|b| < 2^\circ$ the uncertainty in $f(|w_0|)$ due to the declining sample size is also 0.5 km s^{-1} . Hence $|b| < 12^\circ$ represents the best compromise between declining sample size and the corrections described above. The measured velocity distributions for the two samples are also slightly broadened due to errors in the parallaxes and proper motions. However, simulations show that this effect is quite small for our samples. The sample dispersion increases by a mere 0.04 km s^{-1} for the F-stars, and by 0.16 km s^{-1} for the A-stars due to these errors.

The velocity distributions for the two samples, $f(|w_0|)$, are shown in Fig. 3, after a correction for broadening and for the Solar motion relative to the sample stars of $u = 10 \text{ km s}^{-1}$, $v = 10 \text{ km s}^{-1}$ and $w = 7 \text{ km s}^{-1}$. This Solar motion is based on an analysis of the the complete survey and is in good agreement with other determinations based on *Hipparcos* data (Dehnen & Binney 1998; Bienaymé 1999). There are 723 A-stars and 683 F-stars in these two distribution functions. The velocity dispersion of the sample corrected for measurement errors and outliers is $5.7 \pm 0.2 \text{ km}^{-1}$ for the A-stars and $8.3 \pm 0.3 \text{ km}^{-1}$ for the F-stars.

3 DISC MASS MODEL

We determine the local density of matter by comparing the density law of a stellar tracer, predicted from it's vertical velocity distribution at the plane, with the observed density law measured by *Hipparcos*. We follow the method of von Hoerner (1960) in which the distribution of absolute vertical

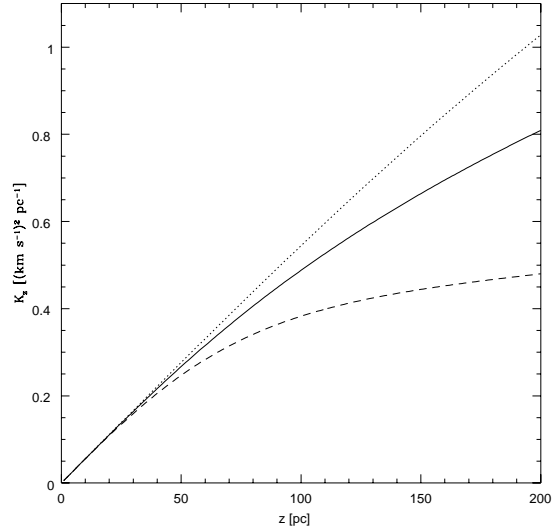


Figure 4. Resulting K_z -force law for three mass models with the same total midplane density of $\rho_0 = 0.103 M_\odot \text{ pc}^{-3}$, of which $0.093 M_\odot \text{ pc}^{-3}$ is in the disc components and $0.01 M_\odot \text{ pc}^{-3}$ is in the dark halo. The solid line shows the reference model from Table 1, the dashed line model is entirely made up of cold gas ($\sigma_z = 4 \text{ km s}^{-1}$) and the dotted line of old stars ($\sigma_z = 20 \text{ km s}^{-1}$).

Table 1. Disc Mass Model

i	Description	$\rho_i(0)$ $M_\odot \text{ pc}^{-3}$	σ_i km s^{-1}	Σ_i $M_\odot \text{ pc}^{-2}$	Note
1	H ₂	0.021	4.0	3.0	C
2	HI(1)	0.016	7.0	4.0	C
3	HI(2)	0.012	9.0	4.0	C
4	warm gas	0.001	40.0	2.0	C
5	giants	0.0006	17.0	0.4	H
6	$M_V < 2.5$	0.0031	7.5	0.9	H
7	$2.5 < M_V < 3.0$	0.0015	10.5	0.6	H
8	$3.0 < M_V < 4.0$	0.0020	14.0	1.1	H
9	$4.0 < M_V < 5.0$	0.0024	19.5	2.0	H
10	$5.0 < M_V < 8.0$	0.0074	20.0	6.5	H
11	$M_V > 8.0$	0.014	20.0	12.3	X
12	white dwarfs	0.005	20.0	4.4	L
13	brown dwarfs	0.008	20.0	6.2	L
14	stellar halo	0.0001	100.0	0.6	L

Notes. C : component constrained by column density
H : component constrained by local density using *Hipparcos*
L : component constrained by local density using star counts
X : component constrained by column density using HST star counts

velocity $f(|w|)$ of the tracer stars at $z = 0$, $f(|w_0|)$, may be used to construct the tracer's vertical density profile in the gravitational potential Φ of the disc (Flynn & Fuchs 1994).

Models for the vertical potential of the Galactic disc are constructed in the manner of Bahcall (1984a,b,c) in which the local visible components of the disc are modeled as isothermal components, specified by a local density and a velocity dispersion. We have made a number of refine-

ments to the mass models of Bahcall because of observational advances since 1984, in particular for the upper main sequence, the giant branch, white dwarfs, red dwarfs and brown dwarfs. The basic model is shown in Table 1, and the resulting K_z -force law is shown in Fig. 4 together with two simple one-component models with the same local density as the reference model.

3.1 Upper main sequence and giant branch

For the main sequence above the turnoff and for giants, *Hipparcos* now provides much improved measurements of the stellar luminosity function. Holmberg et al. (1997) have developed a version of the Bahcall-Soneria Galaxy model with revised luminosity/colour distributions and scale heights which fits the *Hipparcos* Survey data. We have determined the local number density of stars in the absolute magnitude ranges used by Bahcall, for convenient comparison with his models. This affects rows 5 to 9 in Table 1. From our model fitting, there are 0.0013 stars pc^{-3} for $M_V < 2.5$, 0.0010 stars pc^{-3} for $2.5 < M_V < 3.0$, 0.0015 stars pc^{-3} for $3.0 < M_V < 4.0$ and 0.0021 stars pc^{-3} for $4.0 < M_V < 5.0$. For the luminosity range $5.0 < M_V < 8.0$ we take 0.0090 stars pc^{-3} from Jahreiß & Wielen (1997). Adopting the mass-luminosity relation of Henry & McCarthy (1993), we derive the local mass densities ρ_i shown in rows 6 to 10 in Table 1. The local number density of giants is 0.0005 stars pc^{-3} . Adopting a mean mass of 0.9 we derive the local mass density of giants of $0.0006 M_\odot \text{pc}^{-3}$ (row 5 of Table 1); Jahreiß & Wielen (1997) derive the same value also from *Hipparcos*. While the number densities of these components of the model can be accurately determined, there is a large relative error of order 20 per cent in the mass-luminosity conversion in determining individual ρ_i . However, since these stars contribute only about 10 per cent of the local mass, this error has only a minor impact on the total mass model. For these stars the velocity dispersion can be estimated directly using the same technique as for the tracer stars (section 2.2) and are shown as the σ_i in Table 1 in rows 5 to 9. Note that the (*Hipparcos* based) observational data essentially constrain the *local density* and *velocity dispersion* of these stellar types, and this is emphasised by the H in column 6 of Table 1.

3.2 M dwarfs

The column density of disc M dwarfs (Table 1, row 11) can now be measured directly via star counts using HST (Gould, Flynn & Bahcall 1998 and references therein), rather than by extrapolation of the mass function. They measure a column density of M disc dwarfs of $12.3 \pm 1.8 M_\odot \text{pc}^{-2}$. We represent the M dwarfs as a single component with a velocity dispersion of 20km s^{-1} , and we adjust the local density in each model we run to be consistent with a column density of M dwarfs of $12.3 M_\odot \text{pc}^{-2}$. These stars are better constrained observationally by column density than by local density, as indicated by an X in column 6 of Table 1.

3.3 White dwarfs

Several new estimates of white dwarf (WD) number density have been made since 1984. Oswalt et al. (1996), in an analysis of white dwarfs discovered as proper motion companions to main sequence dwarfs, after allowing for the fraction found in binaries, report the space number density $7.6^{+3.7}_{-0.7} \times 10^{-3} \text{pc}^{-3}$. For an adopted WD mass of $0.6 M_\odot$ we have $0.0046 M_\odot \text{pc}^{-3}$. Leggett, Ruiz & Bergeron (1998) find for single WDs in the proper motion survey of Liebert, Dahn & Monet (1988) a space density of $3.4 \times 10^{-3} \text{pc}^{-3}$ or $0.002 M_\odot \text{pc}^{-3}$. Jahreiß & Wielen (1997) report $0.005 M_\odot^{-3}$ for 4 WDs confirmed by *Hipparcos* to be within 5 pc, very close to the Wielen (1974) value of $0.007 M_\odot \text{pc}^{-3}$, which can be compared with that adopted by Bahcall (1984), $0.005 M_\odot \text{pc}^{-3}$. Knox, Hawkins & Hambly (1999) finds $4.16 \times 10^{-3} \text{pc}^{-3}$ or $0.0025 M_\odot \text{pc}^{-3}$. All these estimates are lower limits, since they are based on identified white dwarfs. Interestingly Festin (1998) reports a much higher value of $0.013 M_\odot \text{pc}^{-3}$ for 7 white dwarfs found using the innovative technique of searching against the opaque screens formed by dark molecular clouds in Orion and Ophiuchus. Considering the range of values reported, for the purpose of building mass models we adopt $0.005 M_\odot \text{pc}^{-3}$ but we will consider model WD densities which cover the range $[0.002, 0.013] M_\odot \text{pc}^{-3}$. WDs are primarily constrained by local density measurements as indicated by an L in column 6 of Table 1.

3.4 Brown dwarfs

The long-sought freely floating brown dwarfs (BD) of the old disc have now been found by four groups, namely the Calan-ESO proper motion survey (Ruiz, Leggett & Allard 1997), the DENIS mini survey, (Delfosse et al. 1997), a BRI survey of Irwin, McMahon & Hazard (1991) and UK Schmidt survey of ESO/SERC field 287 (Hawkins et al. 1998). Fuchs, Jahreiß & Flynn (1998) summarize the findings of these groups and the implied minimum densities of BDs in the local disc. The four surveys lead to density estimates of BDs of 0.46pc^{-3} , 0.076pc^{-3} , 0.069pc^{-3} , and 0.15pc^{-3} respectively. Adopting a BD mass of $0.065 M_\odot$ this gives mass densities of $0.03 M_\odot \text{pc}^{-3}$, $0.0049 M_\odot \text{pc}^{-3}$, $0.0045 M_\odot \text{pc}^{-3}$ and $0.01 M_\odot \text{pc}^{-3}$, respectively. These surveys are all in their early stages and promise an accurate accounting of BDs within a few years. A fifth survey, 2MASS, has also reported at least 5 BDs in a 420deg^2 survey (Reid et al. 1998) although it is not possible yet to determine space densities for these BDs. In the model we adopt a BD mass density of $0.008 M_\odot \text{pc}^{-3}$, and consider models over the range of $[0.004, 0.03] M_\odot \text{pc}^{-3}$. BDs are primarily constrained by local density measurements as indicated by an L in column 6 of Table 1.

3.5 Interstellar matter

The remaining component in the model is by far the least well understood. Many studies and compilations exist in the literature on the structure and composition on the multi phase ISM (Hollenbach & Thronson 1987; Combes 1991) which describe a complex mixture, ranging from cold (10K) and dense ($50 M_\odot \text{pc}^{-3}$) dark molecular clouds, to the

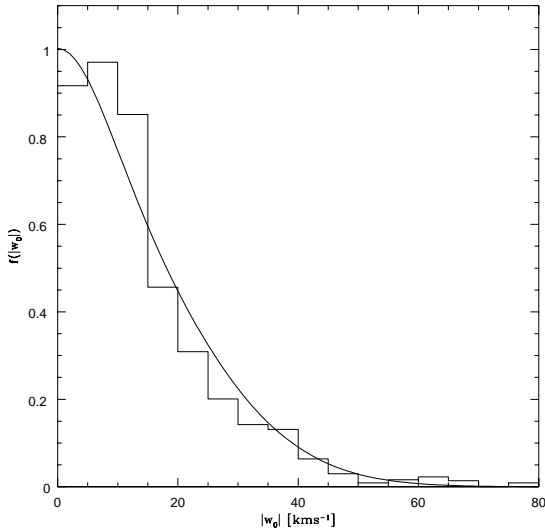


Figure 5. The velocity distribution function for the stellar components of our model (solid line) compared to that observed in the solar neighbourhood by Fuchs & Jahreiß (private communication, histogram).

very hot (10^6 K) and dilute ($0.0001 M_{\odot} \text{ pc}^{-3}$) X-ray emitting coronal gas. Here we adopt the multi-phase model of Bahcall et al. (1992) recognizing that the best determined parameters are the column density and velocity dispersion, which are observable quantities, whereas the deduced local density suffers considerably uncertainties (indicated by a C in column 6 of Table 1). This four-component model consists of $3 M_{\odot} \text{ pc}^{-2}$ at 4 km s^{-1} of molecular gas (Scoville & Sanders 1987), two neutral atomic components each of $4 M_{\odot} \text{ pc}^{-2}$, one cold at 7 km s^{-1} and one warm at 9 km s^{-1} and finally one hot ionized component with $2 M_{\odot} \text{ pc}^{-2}$ at 40 km s^{-1} (Kulkarni & Heiles 1987). The total surface density of these components is about $13 M_{\odot} \text{ pc}^{-2}$, with an uncertainty of about 50 per cent.

3.6 Adopted velocity dispersions

For the early stellar types and giants in the model (rows 5 to 9) the local velocity dispersion σ_i is rather accurate because they are derived from *Hipparcos* data. For all other non-gaseous components the velocity dispersion is not so well determined, and we simply adopt a uniform value of 20 km s^{-1} for what amounts to K to M dwarfs, white dwarfs and brown dwarfs. We are concerned in this paper with using the *Hipparcos* data to measure the local density of matter, whereas the exact choice of σ_i for these components only affects the column density of the models. To illustrate that the adopted value of 20 km s^{-1} is consistent with known constraints, we plot in Fig. 5 the velocity distribution of the combined stellar components in the model (rows 5 to 12 in Table 1) and an observational determination of $f(|w_0|)$ by Fuchs & Jahreiß (private communication) based on *Hipparcos* data for nearby stars. For purposes of determining the local density the match between model and data is suitably accurate.

4 MODEL FITTING AND RESULTS

We now use the velocity distribution functions, $f(|w_0|)$, as determined in section 2.2 for the A- and F-star samples, to predict the density falloff in z of such stars in our disc mass model. The density falloff $\nu(z)$ is determined via the relation (Fuchs & Wielen 1993; Flynn & Fuchs 1994):

$$\nu(z) = 2 \int_{\sqrt{2\Phi}}^{\infty} \frac{f(|w_0|) w_0 dw_0}{\sqrt{w_0^2 - 2\Phi}} \quad (4)$$

where w_0 is the vertical velocity at the mid-plane, $z = 0$ and $\Phi(z)$ is the total gravitational potential generated by the mass model. Equation 4 ignores the radial term in Poisson's equation. If the term is included, Poisson's equation takes the form (Binney & Merrifield 1998):

$$4\pi G\rho = -\frac{\partial K_z}{\partial z} + 2(B^2 - A^2) \quad (5)$$

where A and B are the Oort constants. Using the values derived by Feast & Whitelock (1997), $A = 14.82 \text{ km s}^{-1} \text{ kpc}^{-1}$ and $B = -12.37 \text{ km s}^{-1} \text{ kpc}^{-1}$ the correction term amounts to $-0.0025 M_{\odot} \text{ pc}^{-3}$. However, in a new determination of Mignard (1998) quoted in Kovalovsky (1998), the values are $A = 11.7 \text{ km s}^{-1} \text{ kpc}^{-1}$ and $B = -10.5 \text{ km s}^{-1} \text{ kpc}^{-1}$ giving a smaller correction of $-0.001 M_{\odot} \text{ pc}^{-3}$. These corrections are much smaller than other sources of error, and can be safely neglected.

We integrate Eqn. 4 numerically using the model in Table 1 and the two velocity distribution functions $f(|w_0|)$ shown in Fig. 3 for the A- and F-stars. The integration is performed by using a velocity interval of $\Delta w_0 = 0.01 \text{ km s}^{-1}$ in order to produce a fairly smooth number density falloff — a too large velocity interval (e.g. 0.1 km s^{-1}) causes a visible and non-physical sawtooth effect in the resulting number density law ν .

4.1 A-star sample

The number density falloff for the A-stars resulting from the mass model in Table 1 is shown by the dotted line in Fig. 6, versus the *Hipparcos* data (histogram) and is already seen to be a good fit. We attempted to improve the fit by adding or removing mass from the model, and minimising the difference between the predicted and observed number density as a function of z using a standard χ^2 statistic. It made little difference to the fitting whether this mass was removed proportionally from all rows in the model or (more reasonably) from the most uncertain rows in the model, as one expects since the measurement is so local. For the A-stars the resulting best fitting local density was $\rho_0 = 0.103 \pm 0.006 M_{\odot} \text{ pc}^{-3}$. i.e. just the same as the reference model of Table 1.

4.2 F-star sample

We performed a similar fitting for the F-stars as for the A-stars. For the F stars the best fitting vertical density distribution is shown by the dashed line in Fig. 7, and corresponds to a local density of $\rho_0 = 0.094 \pm 0.017 M_{\odot} \text{ pc}^{-3}$. This best fitting model has slightly less local matter (by approximately 9 per cent) than the basic model in Table 1. As for the A-stars, it made little difference whether the mass

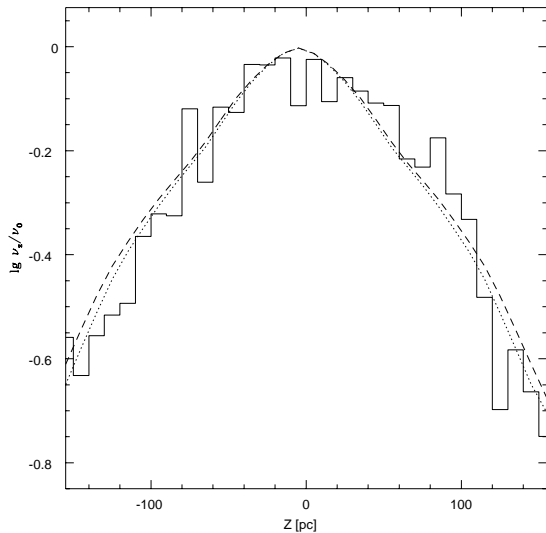


Figure 6. The vertical distribution of A-stars (histogram) versus the prediction of the best fitting mass-model with $\rho_0 = 0.103 M_{\odot} \text{pc}^{-3}$ (dotted line). Also shown is the F-star model with $\rho_0 = 0.094 M_{\odot} \text{pc}^{-3}$ (dashed line).

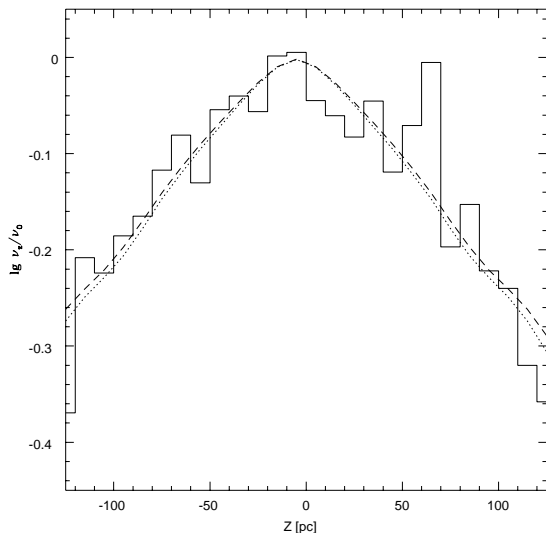


Figure 7. The vertical distribution of F-stars (histogram) versus the prediction of the best fitting mass-model with $\rho_0 = 0.094 M_{\odot} \text{pc}^{-3}$ (dashed line). Also shown is the A-star model with $\rho_0 = 0.103 M_{\odot} \text{pc}^{-3}$ (dotted line)

was removed in proportion from the whole model or from specific rows. To make this best fitting model mass was removed proportionally from the gas and white/brown dwarf components.

4.3 Error estimates

We have estimated our confidence limits via a series of Monte Carlo simulations of observations drawn from syn-

thetic *Hipparcos* survey catalogues. The catalogues were created from a kinematical Galactic model constructed to fit the *Hipparcos* and Tycho catalogues (Holmberg 1999). In each simulation the number density and velocity distribution of the tracer stars was exactly known. A sample was drawn from the simulation taking into account the *Hipparcos* magnitude limits and magnitude dependent parallax and proper motion errors. The local density of the disc was then determined from the artificial sample in the same manner as for the actual data, by measuring $\nu(z)$ and $f(|w_0|)$ and fitting mass models. Several thousand Monte-Carlo simulations of this type allowed us to estimate our confidence limits for a given disc density.

In the modeling of the A-star sample the velocity dispersion was $5.72 \pm 0.18 \text{ km s}^{-1}$ and the best fit density is $\rho_0 = 0.101 \pm 0.006 M_{\odot} \text{pc}^{-3}$, with a 95 per cent confidence limit of $\pm 0.011 M_{\odot} \text{pc}^{-3}$, showing that the uncertainty in the density is totally dominated by the quadratic dependence of the velocity dispersion. The F-star sample had a velocity dispersion of $8.14 \pm 0.24 \text{ km s}^{-1}$ with a best fit density of $\rho_0 = 0.103 \pm 0.017 M_{\odot} \text{pc}^{-3}$, with a 95 per cent confidence limit of $\pm 0.023 M_{\odot} \text{pc}^{-3}$. This shows a differing effect in which the variance of the resulting density is dominated by the uncertainty in the determination of the fall-off of the tracer density.

In the χ^2 fitting process the density distribution resulting from the mass model is considered to be a distribution function without errors. This has the effect that the resulting value of χ^2 is increased by the errors from the velocity distribution function of the tracer stars. In the simulation of the complete sample the mean value of χ^2 was 59.7 instead of the expected 56.3 for a model without errors. For the actual *Hipparcos* samples the resulting values of χ^2 was 77.76 for 57 DF in the total sample, 44.59 for 31 DF in the A-star sample and 33.11 for 25 DF in the F-star sample.

4.4 Disc column density

The total column of gravitating matter in the mass models that best fits all our samples is quite close to the $48 M_{\odot} \text{pc}^{-2}$ of visible matter in our basic disc mass model of Table 1. We strongly emphasize here that our samples are so local that we cannot put any constraints on the column, since most of it is above our tracers. An illustration of this is that if the velocity dispersion of the hot disc stars in the mass model is increased from 20 km s^{-1} to 25 km s^{-1} the column inflates by $7 M_{\odot} \text{pc}^{-2}$ but the local density estimate changes with only $0.002 M_{\odot} \text{pc}^{-3}$ (see also section 3.6 above).

4.5 Dependence on disc mass model

How critical is the formulation of the mass model to the result? We tested this by using the quite different model from Flynn & Fuchs (1994), slightly refined by the inclusion of *Hipparcos* observations (Fuchs 1998, private communication). This model is quite different in that rather than modeling individual mass components by isothermals, as we do here, Flynn & Fuchs reconstructed the disc potential Φ using the velocity distribution function of K and M dwarfs, to which a small component of young stars and gas had been added. Adopting this model for Φ resulted in a change

Table 2. Local density estimates

Density ρ_0 ($M_\odot \text{pc}^{-3}$)	Error ($M_\odot \text{pc}^{-3}$)	Reference
0.185	0.020	Bahcall (1984b)
0.210	0.090	Bahcall (1984c)
0.105	0.015	Bienaymé, Robin & Crézé (1987)
0.260	0.150	Bahcall et al. (1992)
0.110	0.010	Pham (1997)
0.076	0.015	Crézé et al. (1998)
0.102	0.010	This paper
0.150	0.026	Straight average
0.108	0.011	Variance weighted average

of only $0.003 M_\odot \text{pc}^{-3}$ to our best-fitting local mass density determinations.

4.6 Combined A- and F-star sample

Our conclusion in this section is that the dynamically estimated mass in the solar neighbourhood is completely accounted for by the identified material in gas, stars and stellar remnants without any need for dark matter in the disc. Since both the A- and F-star samples agree on the local density within their errors, we combined the sample and derived a best fitting local density of $\rho_0 = 0.102 \pm 0.006 M_\odot \text{pc}^{-3}$, with 95 per cent confidence limits of $\pm 0.010 M_\odot \text{pc}^{-3}$.

4.7 Comparison to other work

Our estimate of the local mass density is $\rho_0 = 0.102 \pm 0.006 M_\odot \text{pc}^{-3}$. From very similar *Hipparcos* data Pham (1997) estimates $\rho_0 = 0.11 \pm 0.01 M_\odot \text{pc}^{-3}$ and Crézé et al. (1998) estimate $\rho_0 = 0.076 \pm 0.015 M_\odot \text{pc}^{-3}$. These estimates differ at less than the $2\text{-}\sigma$ level, but we have investigated possible causes for the discrepancy between them. The major difference between the determinations is the method applied to the data. Pham (1997) used the $2\pi Gh_z^2 \rho_0 = \sigma_z^2$ relation, which implicitly assumes that the tracer stars (i.e. the A- and F-stars) have a Gaussian velocity distribution. Fig. 3 clearly illustrates that this is in fact only an approximation. Had we carried out our analysis using a Gaussian distribution function rather than the measured distribution function $f(|w_0|)$ we would have recovered a local density of $\rho_0 = 0.110 M_\odot \text{pc}^{-3}$. Crézé et al. (1998) estimate the local density by representing the vertical acceleration in the disc K_z by a linear function, $K_z = az$, where a is a constant. K_z may not actually be linear in the region of interest ($z \lesssim 100$ pc). As can be seen in Fig. 4., K_z would not be well represented by a linear function in the model adopted here for all known mass components of the disc (solid line). If we had assumed a strictly linear vertical force law, then tests showed that our best fitting local density would have been reduced to $0.089 M_\odot \text{pc}^{-3}$. This effect could explain part of the difference between our result and Crézé et al. (1998). In summary, the small differences between the three local density estimates using *Hipparcos* data are probably a result of the three different methods used.

Stothers (1998) gives a detailed summary of measurements of the local disc density over more than 60 years since Oort (1932). Stothers draws attention to the fact that there are sufficiently many determinations of ρ_0 that one might apply the central limit theorem and derive the best density from the straight average, which is $0.141 \pm 0.010 M_\odot \text{pc}^{-3}$. However, in contrast to most older studies, almost all determinations from the last 20 years have clearly stated uncertainty estimates attached to the preferred density. The data can be found in Table 2 together with our own estimate in this paper for ρ_0 . The table shows that high estimates of the density generally have large uncertainties. The sample mean weighted by the inverse variance is $0.108 \pm 0.011 M_\odot \text{pc}^{-3}$ which is quite consistent with the *Hipparcos* results. One should note that the last three determinations are based on almost the same data from *Hipparcos*.

5 CONCLUSIONS

From a sample of A and F stars taken from the *Hipparcos* catalogue, we determined vertical space velocities and density distributions. Using a method of von Hoerner (1960) we solved for the vertical potential and hence local density that would give the observed velocity and density distributions. We find that local dynamical mass density of the solar neighbourhood is $0.102 \pm 0.010 M_\odot \text{pc}^{-3}$ well compatible with the identified material in ordinary matter leaving no need for dark matter in the disc. Our estimate is found to be in reasonable agreement with other estimates, taking errors into account. We conclude that there is no compelling evidence for significant amounts of dark matter in the disc.

ACKNOWLEDGMENTS

We thank Burkhard Fuchs, Andy Gould and Lennart Lindgren for many suggestions and comments. We also thank Burkhard Fuchs and Hartmut Jahreiß for allowing us to use their data in advance of publication. JH is supported by the Swedish Space Board. JH also thanks the Finnish Academy for funding several visits to Tuorla Observatory, where part of this work was carried out. This paper is based on data from the ESA *Hipparcos* astrometry satellite.

REFERENCES

- Bahcall J. N., 1984a, ApJ, 276, 156
- Bahcall J. N., 1984b, ApJ, 276, 169
- Bahcall J. N., 1984c, ApJ, 287, 926
- Bahcall J. N., Flynn C., Gould A., 1992, ApJ, 389, 234
- Bienaymé O., Robin A., Crézé M., 1987, A&A, 180,94
- Bienaymé O., 1999, A&A, 341, 86
- Binney J., Merrifield M., 1998, Galactic Astronomy, Princeton University Press
- Combes F., 1991, ARA&A, 29, 195
- Crézé M., Chereul E., Bienaymé O., Pichon C., 1998, A&A, 329, 920
- Dehnen W., Binney J. J., 1998, MNRAS, 298, 387
- Delfosse X. et al, 1997, A&A, 327, L25
- ESA, 1997, The Hipparcos and Tycho Catalogues, ESA SP-1200
- Feast M., Whitelock P., 1997, MNRAS, 291, 683
- Festin L., 1998, A&A, 336, 883

- Flynn C., Fuchs B., 1994, MNRAS, 270, 471
Fuchs B., Wielen R., 1993, in Holt, S. S., Verter, F. eds, Back to the galaxy. AIP Conference Proc. 278, p. 580
Fuchs B., Jahreiss H., Flynn C., 1998, A&A, 339, 405
Gould A., Flynn C., Bahcall J. N., 1998, ApJ, 503, 798
Hakkila J., Myers J. M., Stidham B. J., Hartmann D. H., 1997, AJ, 114, 2043
Hawkins R. S., Ducourant C., Jones H. R. A., Rapaport, M., 1998, MNRAS, 294, 505
Henry T. J., McCarthy D. J. Jr, 1993, AJ, 106, 773
Hollenbach D. J., Thronson H. A., Jr., 1987 Interstellar Processes, Dordrecht Reidel, p. 87
Holmberg J., Flynn C., Lindegren L., 1997, in Perryman M. A. C., Bernacca P. L., eds, HIPPARCOS Venice '97, ESA SP-402, p. 721
Houk N., Swift C. M., Murray C. A., Penston M.J., Binney J. J., 1997, in Perryman M. A. C., Bernacca P. L., eds, HIPPARCOS Venice '97, ESA SP-402, p. 279
Irwin M., McMahon R. G., Hazard C., 1991, in Crampton D., ed., ASP Conf. Ser. Vol. 21, The space distribution of quasars. Astron. Soc. Pac., San Francisco, p. 117
Jahreiß H., Wielen R., 1997, in Perryman M. A. C., Bernacca P. L., eds, HIPPARCOS Venice '97, ESA SP-402, p. 675
Jaschek C., Gómez A., 1998, A&A, 330, 619
Knox R.A., Hawkins M.R.S., Hambly N.C., 1999, MNRAS, 306, 736
Kovalevsky J., 1998, ARA&A, 36, 99
Kuijken K., 1991, ApJ, 372, 125
Kuijken K., Gilmore G., 1989a, MNRAS, 239, 571
Kuijken K., Gilmore G., 1989b, MNRAS, 239, 605
Kuijken K., Gilmore G., 1989c, MNRAS, 239, 651
Kulkarni S. R., Heiles C., 1987, in Hollenbach D. J., Thronson H. A., Jr., eds, Interstellar Processes, Dordrecht, Reidel, p. 87
Leggett S. K., Ruiz M. T., Bergeron P., 1998, ApJ, 497, 294
Liebert J., Dahn C. C., Monet D. G., 1988, ApJ, 332, 891
Mignard, F., 1998, A&A, submitted
Oort J. H., 1932, Bull. Astron. Inst. Netherlands, 6, 249
Oort J. H., 1960, Bull. Astron. Inst. Netherlands, 15, 45
Oswalt T. D., Smith J. A., Wood M. A., Hintzen P., 1995, Nature, 282, 692
Pham H. A., 1997, in Perryman M. A. C., Bernacca P. L., eds, HIPPARCOS Venice '97, ESA SP-402, p. 559
Reid I.N., Kirkpatrick D., Beichman C.A., Liebert J., Burrows A., Skrutskie M., 1998, BAAS, 192, 55.17
Ruiz M. T., Leggett S. K., Allard F., 1997, ApJ, 491, L107
Scoville N. Z., Sanders D. B., 1987, in Hollenbach D. J., Thronson H. A., Jr, eds, Interstellar Processes, Dordrecht, Reidel, p. 87
Stothers, R.B., 1998, MNRAS, 300, 1098
Udry S. et al., 1997, in Perryman M. A. C., Bernacca P. L., eds, HIPPARCOS Venice '97, ESA SP-402, p. 693
von Hoerner S., 1960, Fortschr. Phys., 8, 191
Wielen R., 1974, IAU Highlights of Astronomy, 3, 395
Wielen R., 1977, A&A, 60, 263